CLNS 94/1292
CLEO 94-19

$\Upsilon(1S) \rightarrow \gamma$ + Non-interacting Particles

R. Balest,[1] K. Cho,[1] W.T. Ford,[1] D.R. Johnson,[1] K. Lingel,[1] M. Lohner,[1] P. Rankin,[1] J.G. Smith,[1] J.P. Alexander,[2] C. Bebek,[2] K. Berkelman,[2] K. Bloom,[2] T.E. Browder,[2*] D.G. Cassel,[2] H.A. Cho,[2] D.M. Coffman,[2] D.S. Crowcroft,[2] P.S. Drell,[2] D. Dumas,[2] R. Ehrlich,[2] P. Gaidarev,[2] R.S. Galik,[2] M. Garcia-Sciveres,[2] B. Geiser,[2] B. Gittelman,[2] S.W. Gray,[2] D.L. Hartill,[2] B.K. Heltsley,[2] S. Henderson,[2] C.D. Jones,[2] S.L. Jones,[2] J. Kandaswamy,[2] N. Katayama,[2] P.C. Kim,[2] D.L. Kreinick,[2] G.S. Ludwig,[2] J. Masui,[2] J. Mevissen,[2] N.B. Mistry,[2] C.R. Ng,[2] E. Nordberg,[2] J.R. Patterson,[2] D. Peterson,[2] D. Riley,[2] S. Salman,[2] M. Sapper,[2] F. Würthwein,[2] M. M. Urish,[2] P. Avery,[3] A. Freyberger,[3] J. Rodriguez,[3] S. Yang,[3] J. Yelton,[3] D. Cinabro,[4] T. Liu,[4] M. Saulnier,[4] R. Wilson,[4] H. Yamamoto,[4] T. Bergfeld,[5] B.I. Eisenstein,[5] G. Gollin,[5] B. Ong,[5] M. Palmer,[5] M. Selen,[5] J. J. Thaler,[5] K.W. Edwards,[6] M. Ogg,[6] A. Bellerive,[7] D.I. Britton,[7] E.R.F. Hyatt,[7] D.B. MacFarlane,[7] P.M. Patel,[7] B. Spaan,[7] A.J. Sadoff,[8] R. Ammar,[9] P. Baringer,[9] A. Bean,[9] D. Besson,[9] D. Coppage,[9] N. Copty,[9] R. Davis,[9] N. Hancock,[9] M. Kelly,[9] S. Kotov,[9] I. Kravchenko,[9] N. Kwak,[9] H. Lam,[9] Y. Kubota,[10] M. Lattery,[10] M. Momayezi,[10] J.K. Nelson,[10] S. Patton,[10] R. Poling,[10] V. Savinov,[10] S. Schrenk,[10] R. Wang,[10] M.S. Alam,[11] I.J. Kim,[11] Z. Ling,[11] A.H. Mahmood,[11] J.J. O'Neill,[11] H. Severini,[11] C.R. Sun,[11] F. Wappler,[11] G. Crawford,[12] C. M. Daubenmier,[12] R. Fulton,[12] D. Fujino,[12] K.K. Gan,[12] K. Honscheid,[12] H. Kagan,[12] R. Kass,[12] J. Lee,[12] R. Malchow,[12] M. Sung,[12] C. White,[12] M.M. Zoeller,[12] F. Butler,[13] X. Fu,[13] B. Nemati,[13] W.R. Ross,[13] P. Skubic,[13] M. Wood,[13] M. Bishai,[14] J. Fast,[14] E. Gerndt,[14] R.L. McIlwain,[14] T. Miao,[14] D.H. Miller,[14] M. Modesitt,[14] D. Payne,[14] E.I. Shibata,[14] I.P.J. Shipsey,[14] P.N. Wang,[14] M. Battle,[15] J. Ernst,[15] L. Gibbons,[15] Y. Kwon,[15] S. Roberts,[15] E.H. Thorndike,[15] C.H. Wang,[15] J. Dominick,[16] M. Lambrecht,[16] S. Sanghera,[16] V. Shelkov,[16] T. Skwarnicki,[16] R. Stroynowski,[16] I. Volobouev,[16] G. Wei,[16] P. Zadorozhny,[16] M. Artuso,[17] M. Gao,[17] M. Goldberg,[17] D. He,[17] N. Horwitz,[17] G.C. Moneti,[17] R. Mountain,[17] F. Muheim,[17] Y. Mukhin,[17] S. Playfer,[17] Y. Rozen,[17] S. Stone,[17] X. Xing,[17] G. Zhu,[17] J. Bartelt,[18] S.E. Csorna,[18] Z. Egyed,[18] V. Jain,[18] D. Gibaut,[19] K. Kinoshita,[19] P. Pomianowski,[19] B. Barish,[20] M. Chadha,[20] S. Chan,[20] D.F. Cowen,[20] G. Eigen,[20] J.S. Miller,[20] C. O'Grady,[20] J. Urheim,[20] A.J. Weinstein,[20] M. Athanas,[21] W. Brower,[21] G. Masek,[21] H.P. Paar,[21] M. Sivertz,[21] J. Gronberg,[22] R. Kutschke,[22] S. Menary,[22] R.J. Morrison,[22] S. Nakanishi,[22] H.N. Nelson,[22] T.K. Nelson,[22] C. Qiao,[22] J.D. Richman,[22] A. Ryd,[22] D. Sperka,[22] H. Tajima,[22] and M.S. Witherell[22].

(CLEO Collaboration)

[1] *University of Colorado, Boulder, Colorado 80309-0390*
[2] *Cornell University, Ithaca, New York 14853*
[3] *University of Florida, Gainesville, Florida 32611*
[4] *Harvard University, Cambridge, Massachusetts 02138*
[5] *University of Illinois, Champaign-Urbana, Illinois, 61801*
[6] *Carleton University, Ottawa, Ontario K1S 5B6 and the Institute of Particle Physics, Canada*
[7] *McGill University, Montréal, Québec H3A 2T8 and the Institute of Particle Physics, Canada*
[8] *Ithaca College, Ithaca, New York 14850*
[9] *University of Kansas, Lawrence, Kansas 66045*
[10] *University of Minnesota, Minneapolis, Minnesota 55455*
[11] *State University of New York at Albany, Albany, New York 12222*
[12] *Ohio State University, Columbus, Ohio, 43210*
[13] *University of Oklahoma, Norman, Oklahoma 73019*
[14] *Purdue University, West Lafayette, Indiana 47907*
[15] *University of Rochester, Rochester, New York 14627*
[16] *Southern Methodist University, Dallas, Texas 75275*
[17] *Syracuse University, Syracuse, New York 13244*
[18] *Vanderbilt University, Nashville, Tennessee 37235*
[19] *Virginia Polytechnic Institute and State University, Blacksburg, Virginia, 24061*
[20] *California Institute of Technology, Pasadena, California 91125*
[21] *University of California, San Diego, La Jolla, California 92093*
[22] *University of California, Santa Barbara, California 93106*

(August 11, 1994)

We consider the decay of $\Upsilon(1S)$ particles produced at CESR into a photon which is observed by the CLEO detector plus particles which are not seen. These could be real particles which fall outside of our acceptance, or particles which are non-interacting. We report the results of our search for the process $\Upsilon(1S) \rightarrow \gamma +$"unseen" for photon energies >1 GeV, obtaining limits for the case where "unseen" is either a single particle or a particle-antiparticle pair. Our upper limits represent the highest sensitivity measurements for such decays to date.

---

*Permanent address: University of Hawaii at Manoa

INTRODUCTION

The radiative decays of heavy quarkonia (J/ψ and Υ) offer an opportunity to search for many exotic particles, both within the Standard Model (Higgs bosons [1,2] or glueballs [3]) as well as beyond the Standard Model (axions, [1,2,4], cosmions [5,6] and supersymmetric and other weakly interacting massive particles ("WIMP"'s) [7,8]). For the latter class, the couplings of some of these exotic particles with ordinary matter may be sufficiently weak as to leave no detectable trace in a conventional particle detector. The signature for such exotic radiative decays would therefore be the observation of only a single photon in a detector, with considerable missing energy and momentum.

In some of these cases, such as for axions, the coupling of the undetected particle to quarks can vary with quark species. For the "standard" axion, a_0, in a one Higgs doublet model, the axion-heavy quark couplings are prescribed by a single parameter x, defined as the ratio of the the vacuum expectation values of the charged to neutral Higgs fields. For quarkonia decaying radiatively via $q\bar{q}\rightarrow \gamma + a_0$, the dependence of decay rate on x is proportional to $x^2(x^{-2})$ for charge 2/3(-1/3) constituent quarks. Hence, the product of the decay widths $\Gamma(J/\psi \rightarrow \gamma + a_0) \times \Gamma(\Upsilon \rightarrow \gamma + a_0)$ is independent of x. Based on this, the standard axion has been ruled out by the combined results of radiative ψ and radiative Υ decay [1,9].

The formalism of quark-axion couplings can be extended to other particles. For example, in the same way that there is a U(1) vector gauge boson related to conservation of electric charge, that there may be other U(1) gauge bosons related to the conservation of baryon or lepton number [10,11]. Such a boson could, in principle, effect a neutral current which would be purely vectorial in the simplest case of a single Higgs doublet. However, if there is more than one Higgs doublet (as required by minimal supersymmetric extensions of the Standard Model), such a current acquires an axial component. Such a U(1) gauge boson would then have quarkonium couplings similar to axions through its axial component and could be produced directly in radiative quarkonium decay. The U(1) coupling strength to quarkonium would equal that for axions, but modified by a parameter r, given as the ratio of the electroweak scale (0.25 TeV) relative to the U(1) symmetry-breaking scale. The present Crystal Ball limit on $\Upsilon(1S) \rightarrow \gamma + X$ implies that coupling parameter r should satisfy: $r^2 \leq 1/2$; i.e., the scale of U(1) symmetry breaking is slightly above the electroweak scale.

We present in this paper the result of a search for Υ(1S) decays into a photon plus stable [12], non-interacting particles ("X") using the CLEO-II detector at the Cornell Electron Storage Ring. The scope of the search encompasses both two-body ($\Upsilon \rightarrow \gamma X$) as well as three-body ($\Upsilon \rightarrow \gamma\overline{X}X$) radiative decays. Both the Crystal Ball and ARGUS collaborations have done searches for such decays; the most stringent limit to date on undetected, long-lived particles produced in two-body radiative Υ decay is the upper limit of $\sim 5 \times 10^{-5}$ set by the Crystal Ball collaboration [1].

DETECTOR, DATA SAMPLE AND EVENT SELECTION

The CLEO-II detector is a general purpose solenoidal magnetic spectrometer and calorimeter. Elements of the detector and performance characteristics are described in detail elsewhere [13]. The detector is designed to have high efficiency for triggering and reconstruction of both low-multiplicity as well as high-multiplicity e^+e^- annihilation events. Charged particle momentum measurements are made with three nested cylindrical drift chambers, consisting of 6, 10, and 51 layers of sense wires, respectively. These chambers fill the volume r=4.5 cm to r=92 cm, where r is the radial coordinate relative to the beam axis. Outside the central tracking chambers are plastic scintillation counters which are used as a fast element in the trigger system and also give particle identification information from time of flight measurements. Beyond the time of flight system is the electromagnetic calorimeter, consisting of 7800 thallium-doped CsI crystals. This crystal array gives energy resolution of approximately 4% at 100 MeV, and 1.2% at 5 GeV. The central "barrel" region of the detector covers roughly 80% of the full solid angle. The endcap regions extend the solid angle coverage of the calorimeter to 95% of 4π, albeit with poorer energy resolution than the barrel region. The entire CsI array is subdivided into blocks (16 in the barrel) for triggering purposes; each block is attached to two discriminators. The "low-energy" discriminator turns on a bit in the trigger logic if 100 MeV$< E <$500 MeV is deposited in that trigger block; the "high-energy" discriminator has a threshold corresponding to >500 MeV deposited.

The tracking system, time of flight counters, and calorimeter are contained within a 1.5 T superconducting coil. Flux return and tracking chambers used for muon detection are located immediately outside the coil, in an octagonal geometry, and also in the two endcap regions.

Data Sample and Event Selection

This study examines events taken on the peak of the Υ(1S) resonance in 1992, comprising 48 pb^{-1} of integrated luminosity and corresponding to approximately 960,000 Υ(1S) decays. A special trigger was installed for the Υ(1S) data taking for this study. The trigger line ran at approximately 8 Hz during the data taking; additional cuts were employed in our online software to suppress backgrounds due to cosmic rays and thereby reduce by a factor of 4 the amount of data actually written to tape from this trigger line. Offline software filters were then applied to further suppress backgrounds. The same trigger conditions as were used for the direct photon search at the $\Upsilon(1S)$ energy were also used during runs preceding the Υ(1S) data taking, when we took data at continuum center of mass energies about 1 GeV above the Υ(1S). This off-resonance data set is then used for background studies.

The efficiencies of all the hardware and software selection requirements imposed on our sample are evaluated directly from the data, using $e^+e^- \to \gamma\gamma$, $e^+e^- \to e^+e^-\gamma$, $e^+e^- \to \mu^+\mu^-$ events and random trigger events taken from the same data set.

The cuts imposed, as well as their calculated efficiencies [14] are:

- At the trigger level, we demand that:
  - there be minimal activity in the trigger lines designed to fire if charged tracks are present ($\epsilon = 98.8\pm0.1\%$).
  - there be exactly one "high-energy" trigger bit set in the barrel calorimeter (i.e., deposited energy in a single trigger block exceeding 500 MeV). We designate E_γ as the energy of the shower which fired this trigger bit. Owing to this trigger

requirement, this shower also corresponds to the maximum energy shower in the event. Requiring that there be "exactly" one such shower means that we demand that there be no other 500 MeV trigger bits set in the endcap and no other 100 or 500 MeV trigger bits set in the barrel. The trigger cut is purposely looser in the endcap to allow for the higher backgrounds in the forward regions of the detector. The net efficiency of these calorimeter-based trigger requirements has an energy dependence $F(E_\gamma)$, displayed in Figure 1, which has been determined using photons from $\gamma\gamma$ and $e^+e^-\gamma$ events [15]. Some of this inefficiency arises from cases where the shower is not well contained in one of the 16 crystal trigger blocks of the calorimeter (8 segments in $\phi\times$ 2 segments in z). Energy leakage into an adjacent block can then fire the trigger in that neighboring block. Note that this also introduces a position dependence of the efficiency - e.g., an 800 MeV shower which is pointed at the boundary between two trigger blocks may fail to fire the high-energy discriminator in either block if the deposited energy is distributed equally between them.

A total of 6.56×10^6 events in the $\Upsilon(1S)$ data set satisfied these trigger requirements.

- Online software filtering demands that:
  - there be a low muon chamber occupancy, consistent with single photons and inconsistent with cosmic rays ($\epsilon = 99.9 \pm 0.03\%$).
  - the ratio of energy deposited in the 4 central crystals of the shower with energy E_γ relative to all the energy deposited in the barrel calorimeter (E^{tot}_{shower}) exceeds 0.75; and that the ratio of energy deposited in the 9 central crystals of this shower relative to E^{tot}_{shower} exceeds 0.80 ($\epsilon = 97.1\pm0.2\%$ for $E_\gamma >1.5$ GeV; below 1.5 GeV, the efficiency falls slowly to a value of 0.75 at E_γ=1.0 GeV as the ambient noise level becomes a larger fraction of the total calorimeter energy).

There were a total of 8.6×10^5 events written to tape which satisfied both the trigger as well as the online filter requirements.

- Offline software cuts imposed to reject cosmic rays demand that:
  - the event not have hits concentrated in one octant of the muon chambers, and:
  - hits in the muon chambers not extrapolate to make a match with the most energetic shower in the calorimeter.

These cosmic ray rejection criteria have a measured efficiency of 96.0±0.2%.

- Offline selection of single photon events demands:
  - that the lateral shower shape of the candidate photon be consistent with real photons ($\epsilon = 89.3 \pm 0.2\%$).
  - a stronger restriction on the amount of excess calorimeter activity than that allowed at the trigger level. In particular, we require that the difference: $(E^{tot}_{shower} - E_\gamma)$ <70 MeV ($\epsilon = 85.0\pm0.4\%$).

– that the shower with energy E_γ be confined within the "good" barrel region $|cos\theta_\gamma|$ <0.7, where θ_γ is the polar angle of the shower with respect to the beam axis.

– that the shower not be in a region of the calorimeter known to be subject to spurious electronic noise ($\epsilon = 98.8 \pm 0.1\%$).

For single photon events already contained in the "good" barrel region of the calorimeter, taking into account the correlations between all the cuts imposed, the total event efficiency is thus calculated from the data to be about 39% This is approximately the product of the efficiency function $F(E_\gamma)$ shown in Figure 1 and the effect of the other cuts enumerated above which we use to define our candidate event sample. By comparison, the efficiency as calculated from a full GEANT-based Monte Carlo simulation of the CLEO detector for the radiative decays of interest, including simulation of all trigger efficiencies, is about 2% (absolute) higher than the value we derive from data. The Monte Carlo and data efficiencies therefore agree to within 5% relative to one other.

After imposing all the above requirements, we have suppressed 92.3% of the single photon candidates that were written to tape. Roughly 8.4×10^4 events are left for further analysis. Figure 2 shows the E_γ spectrum for these remaining events.

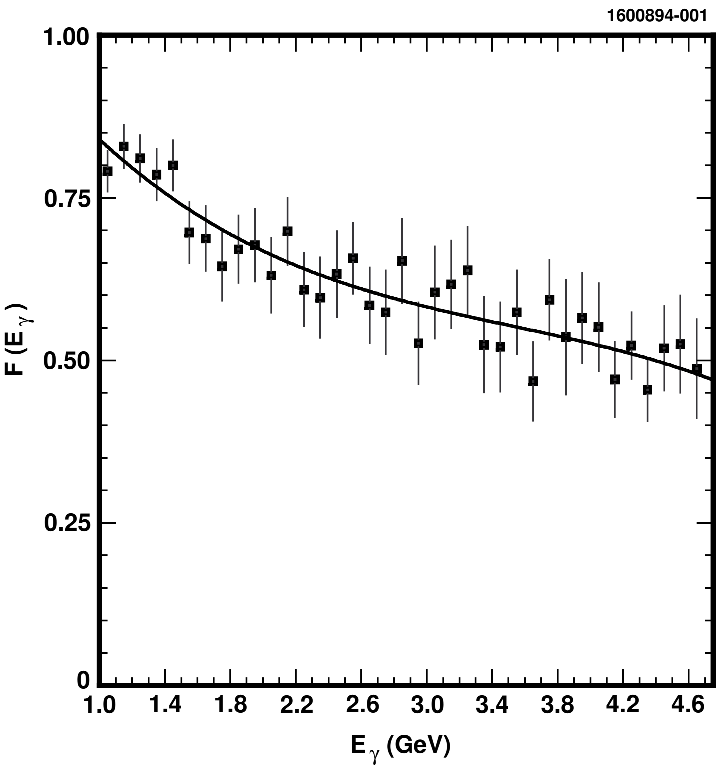

FIG. 1. Efficiency "F(E_γ)", as a function of candidate photon energy for a barrel photon to set exactly one barrel calorimeter trigger bit.

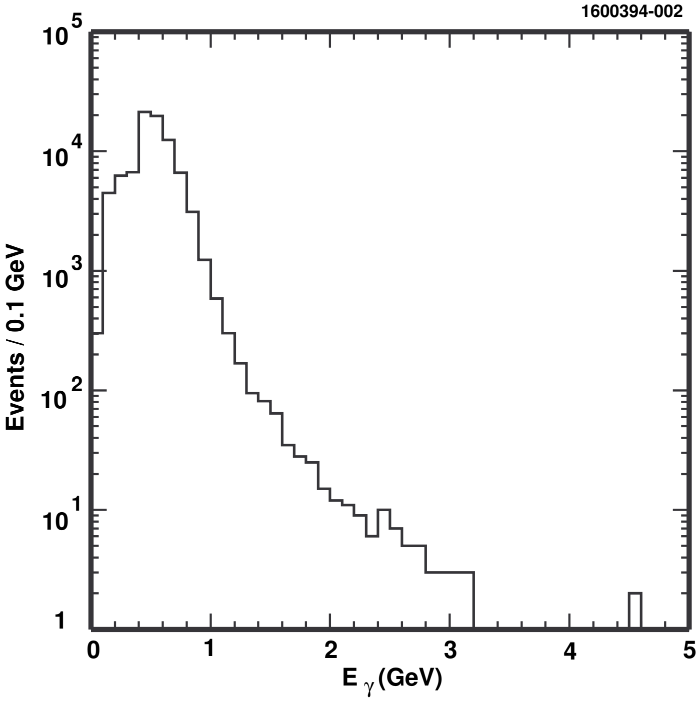

FIG. 2. dN/dE_γ for events passing filter cuts.

Since background processes tend to produce low energy showers, we require that, for further consideration as a candidate signal photon, the most energetic shower have energy in excess of 1 GeV. This photon energy cutoff implies that the maximum mass of X from the three-body process ($\Upsilon(1S) \to \gamma$+X$\bar{\mathrm{X}}$) to which we are sensitive in this study is 4.20 GeV, and that our sensitivity for the two-body case (Υ(1S)$\to$ γ+X) corresponds to 0.0< M_X <8.40 GeV [16].

EVALUATION OF BACKGROUNDS

Aside from the process of interest, there are at least three background processes which we expect to contribute to our candidate event sample. These are cosmic ray backgrounds, backgrounds due to single-beam interactions (beam-wall and beam-gas, e.g.), and QED backgrounds. These processes give showers with quite distinct angular distributions in the detector, and quite different energy spectra.

Cosmic rays which have not yet been rejected by our other cuts are characterized by a multitude of predominantly low-energy clusters in the calorimeter which tend to be aligned along the vertical axis. Such background events are independent of any beam conditions, and depend only on exposure time.

Single beam related backgrounds (beam-wall and beam-gas) are characterized by energy depositions primarily at forward angles with respect to the beam axis. Correspondingly, such events should primarily populate the horizontal plane in azimuth. Such single beam backgrounds depend not on the e^+e^- collision luminosity, but the integrated charge passing through the interaction point (i.e., the single beam currents), and give energy depositions which increase logarithmically with increasing beam energy. We expect, for such backgrounds, that the observed E_γ distribution scales logarithmically with beam energy.

QED backgrounds will arise from $e^+e^- \rightarrow e^+e^-\gamma$ and higher order processes, This background could be due, e.g., to cases where the incident leptons lose some of their energy to a high p_T photon, and emerge with too little transverse momentum to be found within the fiducial volume of the detector. Also possible are cases where a lepton scatters into the fiducial volume of CLEO, but is undetected as a charged track [17]. Assuming no beam polarization in CESR, the resulting shower energy spectrum from QED processes will be isotropic in azimuth, but strongly forward peaked in polar angle. The production cross-section of such QED backgrounds will scale with luminosity and have an energy dependence as $1/s$. We expect the raw energy distribution for such backgrounds to scale with E_{beam}.

The total background from all sources will therefore have some rather complicated dependence on beam energy, beam currents, and CESR luminosity.

Backgrounds are assessed differently in two distinct shower energy regimes. For $1.0 < E_\gamma < 1.5$ GeV, the event count is prohibitively large for scanning, and a statistical subtraction procedure is followed using data taken off the $\Upsilon(1S)$ resonance. These data can then be used as a background sample in evaluating our $1.0 < E_\gamma < 1.5$ GeV signal. However, the unknown fractions of the three types of backgrounds makes it difficult to know *a priori* the proper scale factor to use for the continuum sample. We therefore use an empirical scale factor which is obtained from the data itself, by determining the scale factor required to match the continuum sample to the $\Upsilon(1S)$ sample in the "sideband" photon energy region ($0.5 < E_\gamma <1.0$ GeV), below the signal region.

Comparing the event yields for the on- vs. off-resonance data samples, we find that the scale factor needed to saturate the on-resonance photon spectrum with the off-resonance spectrum in the sideband region is approximately equal to the scale factor that we would calculate if we assumed that the only source of background is from single beam backgrounds. This indicates that single beam effects are, in fact, the primary source of background in this E_γ region. In this case, we expect the distributions to be similar in energy-scaled, as opposed to absolute energy. We therefore perform our subtraction in z ($=E_\gamma/E_{beam}$) as opposed to E_γ, normalizing the continuum data to the $\Upsilon(1S)$ data in the sideband interval ($0.12 < z < 0.20$) [18]. We then apply this scale factor to the signal region ($0.2 < z < 0.3$), and perform the subtraction. The resulting continuum-subtracted z-spectrum is then converted back to E_γ by scaling by E_{beam}, and retained as our candidate signal spectrum for the low photon energy interval.

As a check on the procedure, we have compared the characteristics of the photons selected from the $\Upsilon(1S)$ and continuum data sets. The $\Upsilon(1S)$ and continuum samples show good agreement in the shape of their z spectra. Figure 3 shows the comparison of most energetic shower energy between our resonant data sample and our background data sample after all cuts have been applied (as described above, the two plots have been normalized in the region $0.12 < z < 0.20$). Another notable similarity is found between the $\cos\theta_\gamma$ distributions of the two samples after all cuts have been applied, as shown in Figure 4. The shapes agree

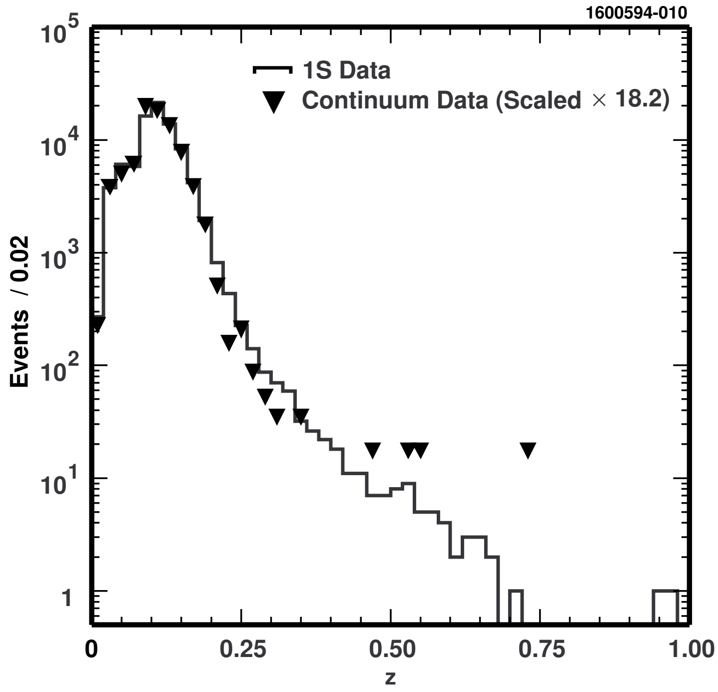

FIG. 3. $z(= E_\gamma/E_{beam})$ in single photon trigger events after applying all cuts.

very well, and show the forward peaking characteristic of beam-related backgrounds. The jaggedness of the $cos\theta_\gamma$ plots results from the previously mentioned position dependence of our calorimeter trigger efficiency, which favors showers at the center and away from the edges of a trigger block.

In the high photon energy region ($E_\gamma > 1.5$ GeV), the event count is sufficiently low after application of cuts that visual scanning of individual events can be done to reject backgrounds. The events passing the cuts up to this point are independently scanned by three physicists. Events containing evidence of excess tracks or showers not detected by our offline software are then flagged as likely background. All events which are classified as background by at least two of the three physicists are rejected from futher consideration. Of the 248 events with E_γ >1.5 GeV, 113 were rejected in scanning [19].

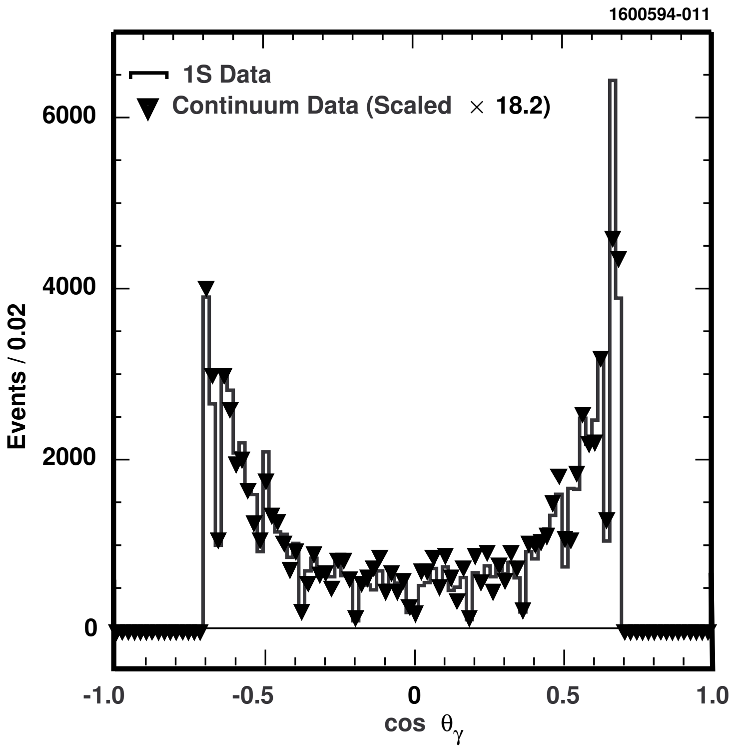

FIG. 4. $\cos\theta_\gamma$ of candidate photons after applying online and offline photon selection cuts.

OBTAINING UPPER LIMITS

Upper Limit for $\Upsilon(1S) \to \gamma X$

High Photon Energies: $E_\gamma > 1.5$ GeV

After scanning, we are left with 135 real single photon event candidates in the interval 1.5-4.7 GeV. The energy distribution of these events is displayed in Figure 5.

We consider all these events as single-photon event candidates. No peaks are observed in the photon energy spectrum; the following procedure is followed to obtain upper limits for the two body decay. For each mass hypothesis, we perform a maximum likelihood fit to a signal Gaussian (with a width fixed to that expected for a single photon in the CLEO-II CsI calorimeter) on top of a smooth low order polynomial background. We use the fitted areas to determine upper limits on the branching ratios. The 90% CL upper limit at each photon energy was obtained by using the area of the fitted Gaussian (taken to be zero if negative) and the uncertainty in that fitted area using the Particle Data Group prescription [3] for probabilities that have physical bounds. For E_γ >2.68 GeV, we simply map the number of events within $\pm 2\sigma$ of the peak bin to a 90% confidence level upper limit; i.e., we assume all events are possible signal. Here, σ is the energy-dependent resolution on the reconstructed shower energy E_γ.

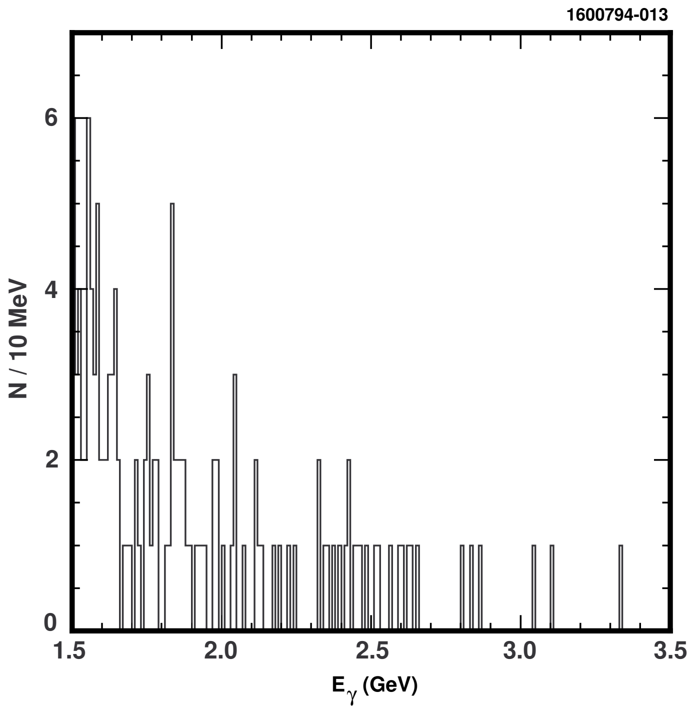

FIG. 5. E_γ distribution of photon candidates (E_γ >1.5 GeV) surviving hardware and software cuts and physicist scanning as described in the text.

Lower Photon Energies: $1.0 < E_\gamma < 1.5$ GeV

Since the raw background shape does not fit a smooth polynomial in this region very well, it is more difficult to fit the raw data to a simple signal plus smooth background in the lower energy regime. For these events, we therefore perform the subtraction as outlined above, using the appropriately scaled continuum data as described previously. After the subtraction, we perform a bin-by-bin χ^2 fit to a Gaussian signal plus lower-order polynomial background, similar to the procedure for the higher energy data sample. Figure 6 displays a typical fit to the data.

Figure 7 shows a plot of our upper limit for the process $\Upsilon(1S) \rightarrow \gamma + X$, where X is any non-interacting particle, as a function of photon energy over the entire region for which we have sensitivity. Systematic errors have been incorporated here into our upper limit by re-calculating the limit using a one sigma downward excursion in our calculated efficiency, taking into account the momentum dependence of this efficiency function. The systematic error is dominated by our uncertainty in the function $F(E_\gamma)$ (2% absolute), and our uncertainty in the offline software filter (5% relative). There is an additional error of 4% which we calculate for our total number of $\Upsilon(1S)$ events (960,000).

For the calculation of the upper limits, we have assumed that the particle X is a pseudoscalar, corresponding to a photon angular distribution of $1 + cos^2\theta$ relative to the beam

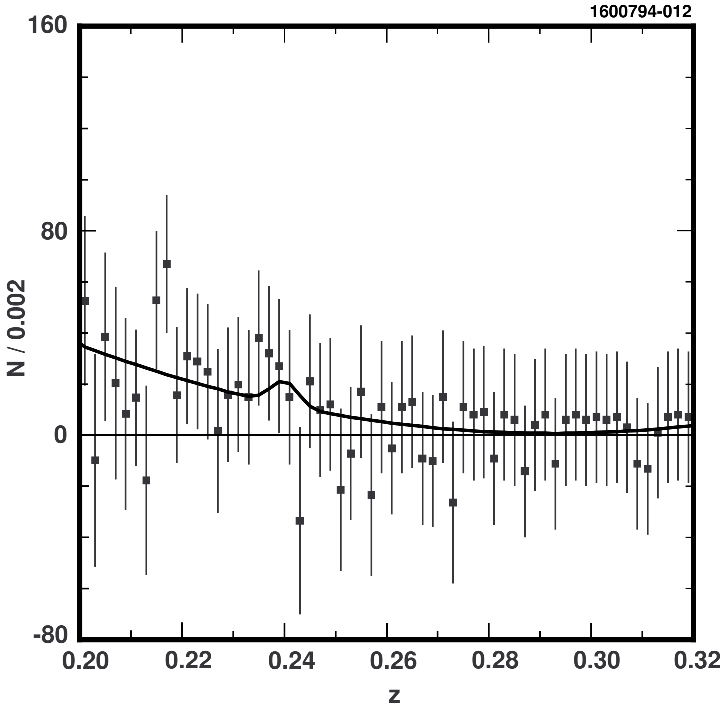

FIG. 6. Fit of background-subtracted candidate photon energy spectrum in $1.0 < E_\gamma < 1.5$ GeV region to a Gaussian signal at 1.14 GeV with the CLEO-II photon resolution plus a polynomial background function.

axis. Our fiducial acceptance under this assumption is 0.61. The CLEO-II limit shown in Figure 7 represents an improvement of the Crystal Ball's limit on the branching ratio of $\leq 5.6 \times 10^{-5}$ [1] over the interval 2.0-4.7 GeV. This is primarily the result of an increased sample size of Υ(1S) events relative to the Crystal Ball data set. Figure 8 displays the same upper limit as a function of X mass.

Upper Limit for Υ(1S)$\rightarrow \gamma\overline{X}X$

We use the scanned event sample only (higher photon energy) to determine the upper limit for a three body decay. In principle, we could follow the same procedure as before by fitting to a signal shape plus a smooth background. Unlike the two-body case, however, for which the true photon energy for a given M_X would be monochromatic, here there is a range of energies that the photon can have, in the interval: $0 < E_\gamma < (\frac{M_\Upsilon^2}{2} - \frac{2M_X^2}{M_\Upsilon})$. One could then generate a phase space spectrum for the photon energies, given a value of M_X and fit the observed data to a sum of that generated phase space spectrum (smeared by experimental resolution, as with the two-body case) plus a smooth background.

A more conservative limit is obtained by assuming all observed events are possible signal

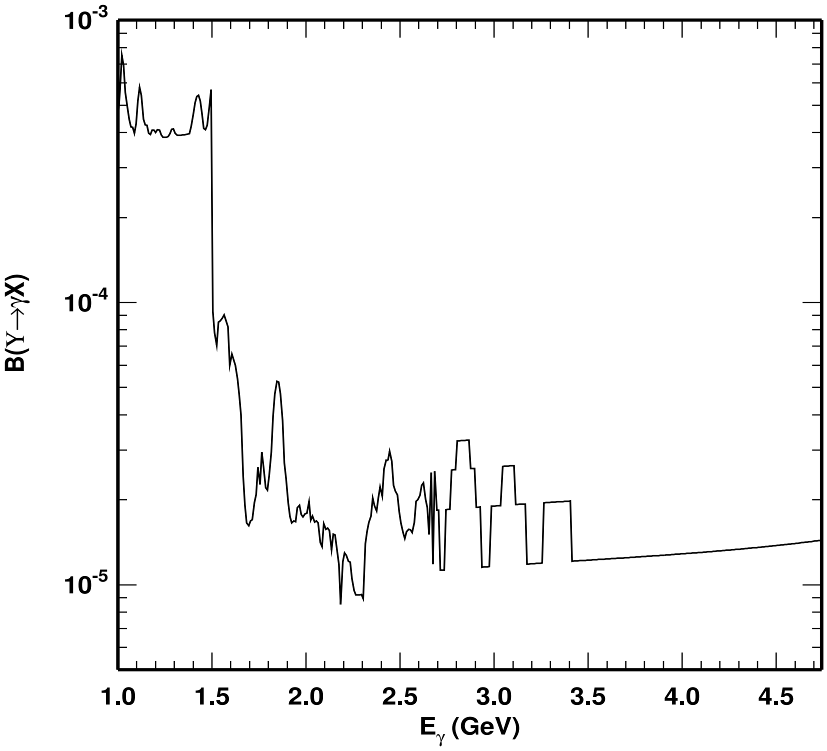

FIG. 7. 90 % C.L. Branching Ratio for $\Upsilon(1S) \rightarrow \gamma X$ as a function of photon energy. (LNS 1600894-008)

and calculating upper limits based on just these observed events. The spectrum observed from the continuum data, which matches the spectrum from the $\Upsilon(1S)$ data very well, as shown in Figure 3, grows exponentially with decreasing photon energy. For a given value of M_X, we therefore restrict our E_γ interval to a region $E_\gamma > E_\gamma^{min}(M_X)$. The minimum photon energy cut E_γ^{min} as a function of M_X is determined according to the following prescription: for each value of M_X, we generate the corresponding photon energy spectrum expected for a phase space three-body decay. The angular acceptance is calculated assuming a spin 1 object, for which the angular distribution as a function of photon momentum has been calculated [20], and is equivalent to the angular distribution of a direct photon in, e.g., Υ(1S)$\rightarrow gg\gamma$. We then empirically determine a minimum photon energy cut $E_\gamma^{min}(M_X)$ which gives the maximum sensitivity to the phase space decay of interest, as a function of X mass. This maximum sensitivity criterion for E_γ^{min} is defined as selecting that cut which optimizes the value of S^2/B, where S is the fraction of signal retained above E_γ^{min}, and B is the amount of background filtering through for our exponentially falling background spectrum, as determined using our off-resonance data sample. We retain events for which $E_\gamma > E_\gamma^{min}(M_X)$. For each value of M_X, we then summed the number of photons in our spectrum from this empirically determined cut up to the appropriate kinematic limit. Taking into account the photon-finding efficiency, along with the fraction of signal we retain, this sum is then mapped to a 90% confidence level upper limit.

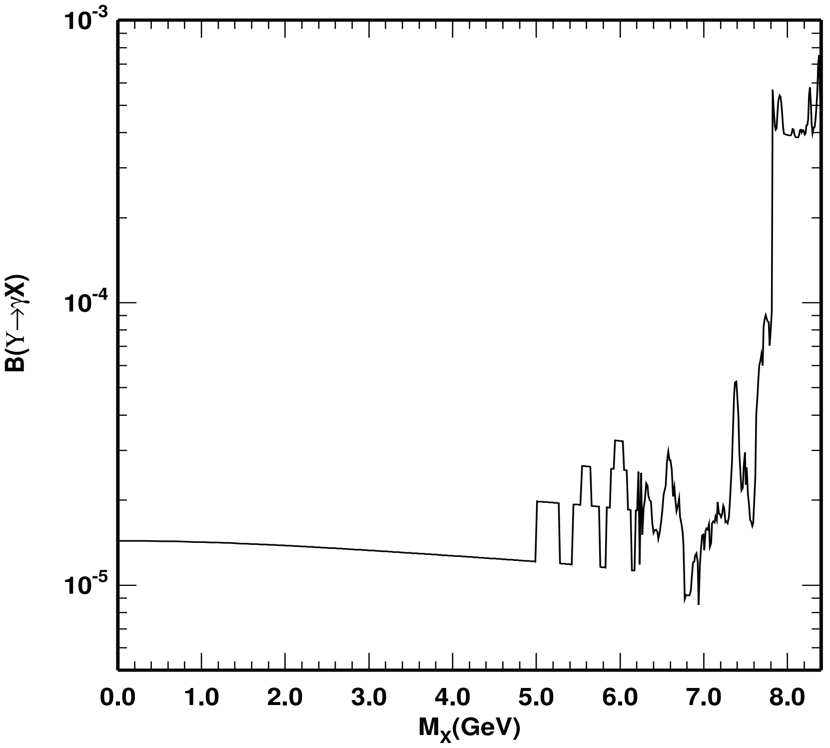

FIG. 8. 90 % C.L. Branching Ratio for $\Upsilon(1S) \to \gamma X$ as a function of X mass, assuming X is a pseudoscalar. (LNS 1600894-009)

Figure 9 shows our 90% confidence level upper limit on the branching ratio for the three body decay, with systematic errors folded into the upper limit as outlined for the two-body case. We obtain upper limits on branching ratios in the range $10^{-5} \to 10^{-3}$ for $0 < M_X < 3.1$ GeV; above 3.1 GeV our limit on the branching ratio climbs steeply because of the poor efficiency for these values of M_X to produce a photon with energies above our minimum photon energy cut.

CONCLUSIONS

Using a sample of approximately one million Υ(1S) decays, we have searched for weakly interacting particles coupling to $b\bar{b}$ quarkonia. For two-body radiative decays of the Υ(1S) into a photon plus some undetected particle, we improved by a factor of two limits set by the Crystal Ball collaboration. For three-body decays of the Υ(1S) resonance into a photon plus some undetected particle X and its antiparticle $\bar{\mathrm{X}}$, we are sensitive at the 10^{-3} branching ratio level, and set upper limits as a function of the mass of the particle X. We find no evidence for non-standard model couplings to bottomonia. If we interpret these results in the context of the "extra" U(1) gauge boson model, we determine that the U(1) symmetry-breaking energy scale is of the order at least twice the electroweak scale.

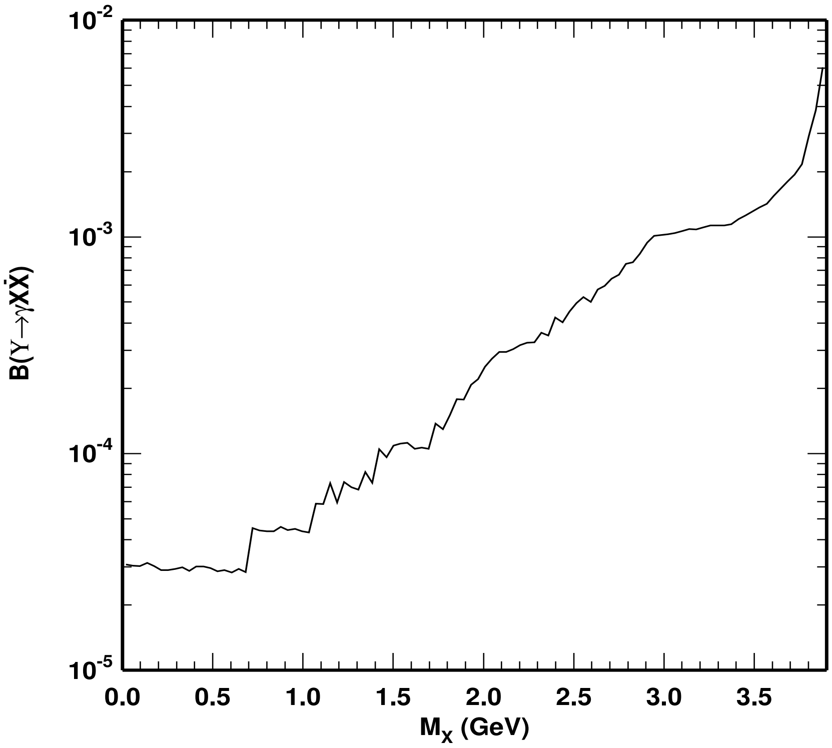

FIG. 9. 90 % C.L. Upper limit to the branching ratio for $\Upsilon(1S) \rightarrow \gamma X\overline{X}$ assuming the decay proceeds via three-body phase space, and assuming that X is a vector particle. In the region between 1.0 and 3.0 GeV, the data approximately fit the form: B(Υ(1S)$\rightarrow \gamma X\bar{X}$)$< 10^{-5} \times exp(1.54 M_X)$, at 90% c.l.. (LNS 1600894-007)

ACKNOWLEDGMENTS

We gratefully acknowledge the effort of the CESR staff in providing us with excellent luminosity and running conditions. This work was supported by the National Science Foundation and the U.S. Dept. of Energy. We also thank Pierre Fayet for illuminating discussions.

[1] D. Antreasyan *et al.* (The Crystal Ball Collaboration), Physics Letters B251, 204 (1990).

[2] H. Albrecht *et al.* (The ARGUS Collaboration), Z. Phys. C42, 349 (1989).

[3] K. Hikasa *et al.*, (PDG) Phys. Rev. D45, 1 (1992).

[4] R.D. Peccei and H.R. Quinn, Phys. Rev. Lett. 38, 1440 (1977), and Phys. Rev. D16, 1791 (1977).

[5] "Cosmion" is a generic term referring to a particle residing in the solar interior that can act as a heat sink and thus lower the temperature of the solar interior sufficiently so as to decrease significantly the production rate of ^8B neutrinos. It should be noted here that recent analyses of the combined Kamiokande and Homestake results mutually exclude core temperature depression as a candidate for the reduced observed neutrino flux, within the context of the Standard Solar Model.

[6] P. Fayet and J. Kaplan, Physics Letters B269, 213 (1991).

[7] D. Besson and T. Skwarnicki, Ann. Rev. Nucl. Part. Sci. 43, 333 (1993).

[8] G. Farrar, private communication, and F. de Campos and J. W. F. Valle, "Possible Implications of a Light Gluino", submitted to the 1993 Intl. Lepton-Photon Symposium, Ithaca, NY USA, FTUV 93-9

[9] C. Edwards, *et al.*, Phys. Rev. Lett. 48, 903 (1982).

[10] P. Fayet, Phys. Lett. B95, 285 (1990), P. Fayet, Nucl. Phys. B187, 184 (1981), and P. Fayet, Phys. Lett. B104, 226 (1981), P. Fayet, Phys. Lett. B84, 421 (1979).

[11] P. Fayet, "New Interactions and the Standard Models", invited talk given at the STEP symposium, Preprint LPTENS 93-24.

[12] We implicitly assume for this paper that the undetected particles being searched for are "stable" in that they would not decay within the volume of the CLEO detector.

[13] Y. Kubota *et al.*, "The CLEO-II detector", Nucl. Instr. Meth. A320, 66 (1992).

[14] The quoted efficiencies are for an individual cut applied to, e.g., the $e^+e^- \to \gamma\gamma$ sample, and do not include correlations between cuts.

[15] This function is plotted taking into account correlations between this efficiency and other losses due to inefficiency; using a sample which has already passed all the other cuts detailed in this section, we plot the fraction of events which satisfy our trigger requirements.

[16] This follows from the relation: $M_X^2 = M_\Upsilon^2 - 2M_\Upsilon E_\gamma$, appropriate for a two-body radiative Υ decay. From this expression, the Crystal Ball minimum energy cut of 2 GeV therefore corresponds to a sensitivity in mass extending up to $M_X \leq$7.2 GeV.

[17] The failure of these events, which generally contain real charged tracks, to register tracking information in the central drift chamber is due to the fact that an event which has had a trigger initiated in the calorimeter reads out data in the drift chamber which is stale. This happens in a very small fraction of those events with real charged tracks (<<1%).

[18] We have considered two possible normalization schemes to determine the continuum scale factor - the first matches the continuum z spectrum to the Υ(1S) sample by normalizing by area; the second determines the scale factor by performing a χ^2 fit. The scale factor that we determine varies by 2%, depending on the choice of normalization. For the former case, the normalization factor obtained is 18.2. When determining final upper limits, we take the

mean of the upper limits calculated using the two normalizations separately, and include the difference between them in the systematic error.
[19] We assess the inefficiency incurred in this scanning procedure by scanning Monte Carlo events into which noise and other effects not related to e^+e^- annihilation have been embedded. The scanning efficiency is estimated by this procedure to be 91%.
[20] K. Koller and T. Walsh, Nucl. Phys. B140, 449 (1978).